

On Steady-State Cornering Equilibria for Wheeled Vehicles with Drift

Efstathios Velenis, Emilio Frazzoli and Panagiotis Tsiotras

Abstract—In this work we derive steady-state cornering conditions for a single-track vehicle model without restricting the operation of the tires to their linear region (i.e. allowing the vehicle to drift). For each steady-state equilibrium we calculate the corresponding tire friction forces at the front and rear tires, as well as the required front steering angle and front and rear wheel longitudinal slip, to maintain constant velocity, turning rate and vehicle sideslip angle. We design a linear controller that stabilizes the vehicle dynamics with respect to the steady-state cornering equilibria using longitudinal slip at the front and the rear wheels as the control inputs. The wheel torques necessary to maintain the given equilibria are calculated and a sliding-mode controller is proposed to stabilize the vehicle using only front and rear wheel torques as control inputs.

I. INTRODUCTION

Stability control for passenger vehicles is usually implemented via differential braking (independent braking control on all four wheels) [1], active steering [2], [3], and, more recently, via integrated chassis control [4], [5], [6]. The latter incorporate and coordinate active chassis systems including differential braking, traction control, active steering and suspension. Alternative means of power transmission for electric and hybrid vehicles have also allowed the development of vehicle stability systems based on independent wheel torque control [7], [8]. The common objective of all of the above systems is to restrict the operation of the vehicle, such that the tires operate within the linear region of the wheel slip-tire friction characteristic, and to match the vehicle's response to that of a simple vehicle model in steady-state cornering [9]. In this way, the average driver can maintain control of the vehicle during an emergency.

Accident avoidance during an emergency may require taking advantage of the full handling capacity of the vehicle, and the employment of expert driving skills, rather than restricting the response of the vehicle. It is envisioned that a new generation of active safety systems will take advantage of the increased situational awareness of modern and future vehicles and use expert driver skills to actively maneuver vehicles away from accidents. With this vision in mind, an analysis of expert driving techniques using nonlinear programming optimization was initiated in [10], [11], [12] and [13]. The driving techniques investigated in these references were those used by rally drivers, which involve

operation of the vehicle outside the stable operation envelope enforced by the current stability systems. The analysis in [10], [11], [12] and [13] provided a significant understanding of the dominant effects during execution of expert driving techniques, but the open-loop approach of the optimization is not implementable in the presence of uncertainties.

A study of the stability of vehicle cornering equilibria with the tires operating at their full range (including linear and nonlinear range) and the design of a stabilizing front wheel steering controller appeared in [14]. The authors of that work used a single-track vehicle model and assumed pure cornering conditions, that is, complete absence of longitudinal forces (tractive or braking) at the wheels. A phase-plane analysis of the cornering equilibria in this work was followed by the design of a linear robust stabilizing steering controller.

The existence of steady-state cornering conditions with excessive vehicle sideslip was demonstrated in [15]. In that reference the author derived explicit steady-state cornering conditions for a single track vehicle model with its tires operating at their full range, using the simplifying assumption of a free rolling rear wheel.

Building on the approach of [15], in this work we allow for the combined cornering and traction/braking tire forces to develop and derive explicit expressions of the steady-state conditions. We design a sliding mode controller using independent wheel torque inputs to stabilize the vehicle with respect to the above steady-states. In the proposed control scheme the steering angle is fixed at its steady-state value, and stabilization is achieved purely by regulation of tractive/braking forces in analogy to well-known and previously studied expert driving techniques [10], [11], [12] and [13].

In the following, we first introduce a single-track model with nonlinear tire characteristics and a static map of longitudinal acceleration to normal load transfer at the wheels. For a given triplet of corner curvature, vehicle speed and sideslip angle, we calculate the necessary front and rear wheel longitudinal slip amounts, and front wheel steering angle, necessary to maintain the steady-state cornering. A linear controller is designed to stabilize the vehicle along the derived equilibria using longitudinal wheel slip control and constant steering angle. The steady-state wheel speeds and the corresponding torques at the front and the rear axles are then calculated, and a sliding mode controller using independent front and rear wheel torque inputs is proposed. A vehicle model of increased fidelity, namely a single-track model with suspension dynamics, is used to demonstrate the efficiency of the controller.

E. Velenis (corresponding author) is with the School of Engineering and Design, Brunel University, Uxbridge, Middlesex, UB8-3PH, UK, Email: efstathios.velenis@brunel.ac.uk

E. Frazzoli is with the Department of Aeronautics and Astronautics, Massachusetts Institute of Technology, Cambridge, MA 02139, USA, Email: frazzoli@mit.edu

P. Tsiotras is with the Daniel Guggenheim School of Aerospace Engineering, Georgia Institute of Technology, Atlanta, GA 30332-0150, USA, Email: tsiotras@gatech.edu

II. VEHICLE MODEL

In this section we introduce a single-track vehicle model with nonlinear tire characteristics. We employ a static map to calculate the normal load transfer from front to rear wheels, and vice-versa, arising from the longitudinal acceleration of the vehicle.

A. Equations of Motion of the Single-Track Model

The equations of motion of the single-track model (Fig. 1) may be expressed in a body-fixed frame with the origin at the vehicle's center of mass (C.M.) as follows:

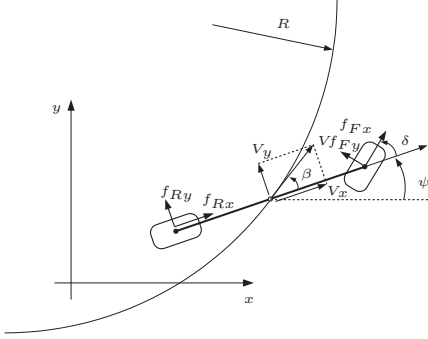


Fig. 1. Single-track vehicle model.

$$m(\dot{V}_x - V_y \dot{\psi}) = f_{Fx} \cos \delta - f_{Fy} \sin \delta + f_{Rx}, \quad (1)$$

$$m(\dot{V}_y + V_x \dot{\psi}) = f_{Fx} \sin \delta + f_{Fy} \cos \delta + f_{Ry}, \quad (2)$$

$$I_z \ddot{\psi} = (f_{Fy} \cos \delta + f_{Fx} \sin \delta) \ell_F - f_{Ry} \ell_R, \quad (3)$$

where $V_x = V \cos \beta$, $V_y = V \sin \beta$. In the above equations m is the vehicle's mass, I_z is the polar moment of inertia of the vehicle, V_x and V_y are the body-frame components of the vehicle velocity V , ψ is the yaw angle of the vehicle, and δ is the steering angle of the front wheel. By f_{ij} ($i = F, R$ and $j = x, y$) we denote the longitudinal and lateral friction forces at the front and rear wheels, respectively. The vehicle sideslip angle is given by $\beta = \tan^{-1}(V_y/V_x)$.

B. Tire Forces

In [16] the theoretical longitudinal and lateral slip quantities are defined, respectively, as:

$$s_{ix} = \frac{V_{ix} - \omega_i r_i}{\omega_i r_i}, \quad s_{iy} = \frac{V_{iy}}{\omega_i r_i} = (1 + s_{ix}) \tan \alpha_i.$$

where the index $i = F, R$ denotes the front and rear axle of the single-track model respectively, ω_i is the rotational speed of the wheel, r_i is the wheel radius, and V_{ij} , ($i = F, R$, $j = x, y$) are the tire frame components of the vehicle body velocity vector at the front and rear axles. The slip angle at each wheel is given by $\tan \alpha_i = V_{iy}/V_{ix}$. The overall, or total, slip at each tire is defined by $s_i = \sqrt{s_{ix}^2 + s_{iy}^2}$.

The relative velocities of the front and rear wheels of the single-track model along each wheel's longitudinal and lateral axes are given by:

$$V_{Fx} = V \cos(\beta - \delta) + \dot{\psi} \ell_f \sin \delta, \quad V_{Rx} = V \cos(\beta), \\ V_{Fy} = V \sin(\beta - \delta) + \dot{\psi} \ell_f \cos \delta, \quad V_{Ry} = V \sin(\beta) - \dot{\psi} \ell_R.$$

Assuming linear dependence of the tire friction forces on the tire normal force, we obtain

$$\mu_i = f_i/f_{iz}, \quad \mu_{ij} = f_{ij}/f_{iz}, \quad i = F, R, \quad j = x, y, \quad (4)$$

where $f_i = \sqrt{f_{ix}^2 + f_{iy}^2}$ is the total friction force at each tire, μ_i is the total friction coefficient, μ_{ij} are the longitudinal and lateral friction coefficients, and f_{iz} are the normal loads at the front and rear tires.

We calculate the total friction coefficient using Pacejka's "magic formula" (MF) [16] as follows:

$$\mu_i(s_i) = \text{MF}(s_i) = D \sin(C \operatorname{atan}(B s_i)).$$

Assuming symmetric tire characteristics, with respect to the longitudinal and lateral directions, the total friction force for each tire lies within the so-called friction circle. In this case, the tire friction force components are given by:

$$\mu_{ij} = -(s_{ij}/s_i) \mu(s_i). \quad (5)$$

Neglecting suspension dynamics, the equilibrium of forces in the vertical direction and the equilibrium of moments about the body- y axis are used to find front and rear axle normal loads:

$$0 = h(f_{Fx} \cos \delta - f_{Fy} \sin \delta + f_{Rx}) + f_{Fz} \ell_F - f_{Rz} \ell_R, \quad (6)$$

$$0 = f_{Fz} + f_{Rz} - mg, \quad (7)$$

where h is the height of C.M. from the road surface.

III. STEADY-STATE CORNERING CONDITIONS

In this section we derive steady-state cornering conditions for the vehicle model of the previous section. For a given corner curvature, vehicle speed and sideslip angle, we calculate the corresponding tire friction forces of the front and rear wheels.

Steady-state cornering is characterized by a trajectory of constant radius R , negotiated at a constant speed V , and constant yaw rate and slip angle:

$$R = R^{ss}, \quad V = V^{ss}, \quad \dot{\psi} = \dot{\psi}^{ss} = \frac{V^{ss}}{R^{ss}}, \quad \beta = \beta^{ss}.$$

Under steady-state cornering conditions, equations (1), (2), (3), (6) and (7) are summarized below:

$$0 = f_{Fx}^{ss} \cos \delta^{ss} - f_{Fy}^{ss} \sin \delta^{ss} + f_{Rx}^{ss} \\ - \frac{m(V^{ss})^2}{R^{ss}} \sin \beta^{ss}, \quad (8)$$

$$0 = f_{Fx}^{ss} \sin \delta^{ss} + f_{Fy}^{ss} \cos \delta^{ss} + f_{Ry}^{ss} \\ - \frac{m(V^{ss})^2}{R^{ss}} \cos \beta^{ss}, \quad (9)$$

$$0 = (f_{Fx}^{ss} \sin \delta^{ss} + f_{Fy}^{ss} \cos \delta^{ss}) \ell_F - f_{Ry}^{ss} \ell_R, \quad (10)$$

$$0 = f_{Fz}^{ss} + f_{Rz}^{ss} - mg, \quad (11)$$

$$0 = h(f_{Fx}^{ss} \cos \delta^{ss} - f_{Fy}^{ss} \sin \delta^{ss} + f_{Rx}^{ss}) \\ + f_{Fz}^{ss} \ell_F - f_{Rz}^{ss} \ell_R. \quad (12)$$

In the following, we derive the conditions that the rear and front wheel slip s_{ij} ($i = F, R$, $j = x, y$), and the corresponding wheel forces f_{ij} , need to satisfy in order for the vehicle to maintain a steady-state condition defined by the triplet $(V^{ss}, R^{ss}, \beta^{ss})$.

A. Rear Axle Steady-State Equations

Equations (9) and (10) can be solved for f_{Ry} as a function of V^{ss} , R^{ss} , and β^{ss} , resulting in

$$f_{Ry}^{ss} = \frac{m(V^{ss})^2}{R^{ss}} \cos \beta^{ss} \frac{\ell_F}{\ell_F + \ell_R}.$$

Equations (8), (11) and (12) lead to the following expressions for the front and rear axle normal loads as functions of V^{ss} , R^{ss} and β^{ss} :

$$f_{Rz}^{ss} = \frac{mg\ell_F - mh(V^{ss})^2 \sin \beta^{ss}/R^{ss}}{\ell_F + \ell_R}, \quad (13)$$

$$f_{Fz}^{ss} = \frac{mg\ell_R + mh(V^{ss})^2 \sin \beta^{ss}/R^{ss}}{\ell_F + \ell_R}. \quad (14)$$

Hence, given V^{ss} , R^{ss} and β^{ss} we can compute the steady-state μ_{Ry}^{ss} from $\mu_{Ry}^{ss} = f_{Ry}^{ss}/f_{Rz}^{ss}$, as well as $\tan(\alpha_R^{ss})$, from

$$\tan(\alpha_R^{ss}) = \frac{V^{ss} \sin \beta^{ss} - V^{ss} \ell_R/R^{ss}}{V^{ss} \cos \beta^{ss}}.$$

Pacejka's Magic formula and the slip definitions result in the following three equations with three unknowns, namely s_R^{ss} , s_{Rx}^{ss} and s_{Ry}^{ss} :

$$\tan(\alpha_R^{ss}) = s_{Ry}^{ss}/(1 + s_{Rx}^{ss}), \quad (15)$$

$$s_R^{ss} = \sqrt{(s_{Rx}^{ss})^2 + (s_{Ry}^{ss})^2}, \quad (16)$$

$$\mu_{Ry}^{ss} = -(s_{Ry}^{ss}/s_R^{ss})\text{MF}(s_R^{ss}). \quad (17)$$

Solving equations (15), (16) and (17) for the rear tire slip quantities, finally leads to the computation of the longitudinal friction force at the rear wheel:

$$f_{Rx}^{ss} = \mu_{Rx}^{ss} f_{Fz}^{ss}, \quad \mu_{Rx}^{ss} = -\frac{s_{Rx}^{ss}}{s_{Ry}^{ss}} \mu_{Ry}^{ss}, \quad \mu_R^{ss} = \text{MF}(s_R^{ss}).$$

B. Front Axle Steady-State Equations

Equations (8) and (9) result in the following calculation of the total front axle friction force, as a function of the rear axle forces and the steady-state triplet $(R^{ss}, V^{ss}, \beta^{ss})$:

$$f_F^{ss} = \left(\frac{m^2(V^{ss})^4}{(R^{ss})^2} + (f_{Rx}^{ss})^2 + (f_{Ry}^{ss})^2 + 2 \frac{m(V^{ss})^2}{R^{ss}} (f_{Rx}^{ss} \sin \beta^{ss} - f_{Ry}^{ss} \cos \beta^{ss}) \right)^{\frac{1}{2}}.$$

Given the front axle normal load from (13), we also get

$$\mu_F^{ss} = f_F^{ss}/f_{Fz}^{ss}, \quad s_F^{ss} = \text{MF}^{-1}(\mu_F^{ss}).$$

Applying the friction circle equation (5) and the friction coefficient definition (4) at the front axle forces in equation (8) results in:

$$\frac{(V^{ss})^2}{R^{ss}} = \frac{(f_F^{ss}/s_F^{ss})(s_{Fx}^{ss} \cos \delta^{ss} - s_{Fy}^{ss} \sin \delta^{ss}) - f_{Rx}^{ss}}{m \sin \beta^{ss}}. \quad (18)$$

Recalling the definitions of front lateral slip and total front slip

$$\frac{s_{Fy}^{ss}}{1 + s_{Fx}^{ss}} = \frac{V^{ss} \sin(\beta^{ss} - \delta^{ss}) + V^{ss} \ell_F \cos \delta^{ss}/R^{ss}}{V^{ss} \cos(\beta^{ss} - \delta^{ss}) + V^{ss} \ell_F \sin \delta^{ss}/R^{ss}}, \quad (19)$$

$$s_F^{ss} = \sqrt{(s_{Fx}^{ss})^2 + (s_{Fy}^{ss})^2}, \quad (20)$$

and solving equations (18)-(20) for the front tire slip quantities and steering angle, leads finally to the computation of the longitudinal and lateral friction forces at the front wheel:

$$f_{Fj}^{ss} = -(s_{Fj}^{ss}/s_F^{ss})\text{MF}(s_F^{ss})f_{Fz}^{ss}, \quad j = x, y.$$

IV. CORNERING CONTROL USING TIRE SLIP

In this section we design an LQR stabilizing controller using purely longitudinal control, that is, assuming front and rear wheel longitudinal slips s_{Fx} and s_{Rx} as control inputs. We consider the steering angle δ as a parameter fixed to its steady-state value as calculated above.

We first express the equations of motion of the single-track model (1)-(3) in terms of the state variables V , β and ψ :

$$\begin{aligned} \frac{d}{dt} V &= f_1(V, \beta, \psi, s_{Fx}, s_{Rx}) = \\ &= \frac{1}{m} [f_{Fx} \cos(\delta - \beta) - f_{Fy} \sin(\delta - \beta) \\ &\quad + f_{Rx} \cos \beta + f_{Ry} \sin \beta], \end{aligned} \quad (21)$$

$$\begin{aligned} \frac{d}{dt} \beta &= f_2(V, \beta, \psi, s_{Fx}, s_{Rx}) = \\ &= \frac{1}{mV} [f_{Fx} \sin(\delta - \beta) + f_{Fy} \cos(\delta - \beta) \\ &\quad - f_{Rx} \sin \beta + f_{Ry} \cos \beta - mV\dot{\psi}], \end{aligned} \quad (22)$$

$$\begin{aligned} \frac{d}{dt} \psi &= f_3(V, \beta, \psi, s_{Fx}, s_{Rx}) = \\ &= \frac{\ell_F}{I_z} [f_{Fy} \cos \delta + f_{Fx} \sin \delta] - \frac{\ell_R}{I_z} f_{Ry}. \end{aligned} \quad (23)$$

The steady-state triplet $(R^{ss}, V^{ss}, \beta^{ss})$ results in the equilibrium point $(V^{ss}, \beta^{ss}, \psi^{ss} = V^{ss}/R^{ss})$ of the above equations, that is

$$f_i(V^{ss}, \beta^{ss}, \psi^{ss}, s_{Fx}^{ss}, s_{Rx}^{ss}) = 0, \quad i = 1, 2, 3,$$

where s_{ix}^{ss} ($i = F, R$) are the steady-state front and rear wheel longitudinal slips, as calculated in Sections III-A and III-B.

Equations (21)-(23) can now be linearized as follows

$$\frac{d\tilde{x}}{dt} = \mathcal{A}^{ss} \tilde{x} + \mathcal{B}^{ss} \tilde{u}, \quad \tilde{y} = \mathcal{C} \tilde{x},$$

where \mathcal{A}^{ss} and \mathcal{B}^{ss} are the Jacobian matrices (with respect to the vehicle's state and slip inputs), computed at the equilibrium point $(V^{ss}, \beta^{ss}, \psi^{ss})$, and

$$\tilde{x} = \begin{bmatrix} V - V^{ss} \\ \beta - \beta^{ss} \\ \psi - \psi^{ss} \end{bmatrix}, \quad \tilde{u} = \begin{bmatrix} s_{Fx} - s_{Fx}^{ss} \\ s_{Rx} - s_{Rx}^{ss} \end{bmatrix}, \quad \mathcal{C} = \mathcal{I}^{3 \times 3}.$$

The control law

$$\tilde{u} = -\mathcal{K} \tilde{x}, \quad (24)$$

where the control gain matrix is given by $\mathcal{K} = \mathcal{R}^{-1}(\mathcal{B}^{ss})^T \mathcal{P}$, and \mathcal{P} is the symmetric positive-definite solution to the following algebraic Riccati equation

$$(\mathcal{A}^{ss})^T \mathcal{P} + \mathcal{P} \mathcal{A}^{ss} - \mathcal{P} \mathcal{B}^{ss} \mathcal{R}^{-1} (\mathcal{B}^{ss})^T \mathcal{P} + \mathcal{C}^T \mathcal{Q} \mathcal{C} = 0,$$

stabilizes the equilibrium $\tilde{x} = [0 \ 0 \ 0]^T$ and minimizes the quadratic cost

$$\mathcal{J} = \int_0^\infty [\tilde{y}(t)^T \mathcal{Q} \tilde{y}(t) + \tilde{u}(t)^T \mathcal{R} \tilde{u}(t)] dt.$$

The matrix \mathcal{Q} is real, symmetric and positive semi-definite, and matrix \mathcal{R} is real, symmetric and positive definite.

V. STEADY-STATE WHEEL SPEEDS AND TORQUE INPUTS

In Sections III-A and III-B we calculated the front and rear tire forces f_{ij}^{ss} , ($i = F, R$, $j = x, y, z$), the associated tire slip quantities s_{ij}^{ss} , ($i = F, R$, $j = x, y$) and the front wheel steering angle δ^{ss} required to maintain a steady-state triplet $(R^{\text{ss}}, V^{\text{ss}}, \beta^{\text{ss}})$. Next, we calculate the steady-state wheel speeds ω_i^{ss} , ($i = F, R$) and input wheel torques T_i^{ss} , ($i = F, R$).

From the definition of the longitudinal wheel slip we find:

$$\omega_F = \frac{V_{Fx}}{(1 + s_{Fx})r} = \frac{V \cos(\beta - \delta) + \dot{\psi} \ell_F \sin \delta}{(1 + s_{Fx})r}, \quad (25)$$

$$\omega_R = \frac{V_{Rx}}{(1 + s_{Rx})r} = \frac{V \cos \beta}{(1 + s_{Rx})r}. \quad (26)$$

The equation describing the rotation of the wheels is as follows:

$$I_{wi} \dot{\omega}_i = T_i - f_{ix} r_i, \quad i = F, R, \quad (27)$$

where I_{wi} ($i = F, R$) is the moment of inertia of each wheel about its axis of rotation, r_i ($i = F, R$) is the radius of each wheel and T_i is the driving/braking torque applied at each wheel. In steady-state motion the wheel speeds maintain constant values as in (25) and (26), thus equation (27) can be used to calculate the steady-state torques at each wheel:

$$T_i^{\text{ss}} = f_{ix}^{\text{ss}} r_i, \quad i = F, R.$$

A. Steady-State Conditions Using Wheel Torque Inputs

In this section we present steady-state cornering conditions over several fixed corner radii, a range of vehicle speeds and a range of vehicle sideslip angles. For a given steady-state triplet $(R^{\text{ss}}, V^{\text{ss}}, \beta^{\text{ss}})$, we seek the steady-state slip quantities, steering angle and tire friction forces at the front and rear tires using the derivations of Sections III-A and III-B. In addition, we calculate the steady-state torque inputs using the derivations of Section V. The parameters of the vehicle used for the calculations are given in Table I.

In Table II we present a number of the steady-state conditions including the values of steady-state steering angle and front and rear wheel torques. We observe that multiple steady-states corresponding to the same radius and vehicle speed are possible, as revealed by cases (a) and (b) in Table II. If we were to consider more traditional types of transmission, such as front-, rear-, and all-wheel-drive (FWD, RWD and AWD) we would need to classify these steady-states according to their feasibility with respect to a specific type of transmission. For instance, we notice that for the steady-state conditions (c), (e) and (g) the input torques satisfy $T_F^{\text{ss}} \geq T_R^{\text{ss}} \geq 0$, which are not achievable by a

FWD or a RWD vehicle. The above steady-states require both front and rear powered wheels (AWD) with appropriate torque distribution, or the simultaneous application of throttle and handbrake to reduce the rear wheel torque. On the other hand, for the steady-state conditions (d), (f) and (h) the input torques satisfy $T_F^{\text{ss}} \leq 0$ and $T_R^{\text{ss}} \geq 0$, which are not achievable by a FWD vehicle. This classification of the steady-state equilibria according to the require wheel torques will be considered in a future research of this subject.

TABLE I
Vehicle Parameters.

| m (kg) | I_z (kg m ²) | ℓ_F (m) | ℓ_R (m) | h (m) | I_{wF} (kgm ²) |
|-----------|----------------------------|--------------|--------------|---------|------------------------------|
| 1450 | 2741.9 | 1.1 | 1.59 | 0.4 | 1.8 |
| r_F (m) | r_R (m) | B | C | D | I_{wR} (kgm ²) |
| 0.3 | 0.3 | 7 | 1.6 | 1 | 1.8 |

TABLE II

Steady-state cornering conditions and associated torque and steering inputs.

| Case | R^{ss} (m) | V^{ss} (m/s) | β^{ss} (deg) | T_F^{ss} (Nm) | T_R^{ss} (Nm) | δ^{ss} (deg) |
|------|---------------------|-----------------------|---------------------------|------------------------|------------------------|----------------------------|
| (a) | 7 | 7 | -10.4 | -543 | 1194 | 3.2 |
| (b) | 7 | 7 | -51 | -56 | 1471 | -40.7 |
| (c) | 7 | 8 | -14 | 856 | 673 | -13.7 |
| (d) | 7 | 8.3 | -2 | -106 | 401 | -3.3 |
| (e) | 15 | 12 | -14 | 1058 | 793 | -20.6 |
| (f) | 15 | 11.7 | -6 | -49 | 877 | -9.9 |
| (g) | 1.5 | 3.5 | -40 | 1175 | 1149 | 0.5 |
| (h) | 1.5 | 3.45 | -17 | -273 | 612 | 19.4 |

VI. STABILIZATION OF STEADY-STATE CORNERING VIA SLIDING-MODE CONTROL

In this section we design a sliding-mode control scheme to stabilize the vehicle with respect to steady-state equilibria incorporating the wheel speed dynamics, and using independent front and rear wheel torque control.

Consider the system (21)-(23) complemented by the dynamics of the rotating front and rear wheels (27). Recall that for a given operating condition of the vehicle $(V, \beta, \dot{\psi})$, a reference pair of front and rear longitudinal slip quantities s_{Fx} and s_{Rx} correspond to reference front and rear wheel speeds ω_F and ω_R , as in (25) and (26), respectively.

Define

$$\tilde{z}_i = \omega_i - \phi_i(V, \beta, \dot{\psi}), \quad i = F, R, \quad (28)$$

where $\phi_i(V, \beta, \dot{\psi}) = V_{ix}/(r + s_{ix}r)$, and the slip quantities s_{ix} are given by the stabilizing control law (24).

Equation (28) results in

$$\begin{aligned} \dot{\tilde{z}}_i &= \frac{1}{I_w} T_i - \frac{r}{I_w} f_{ix} - \frac{\partial \phi_i}{\partial V} f_1(V, \beta, \dot{\psi}) \\ &\quad - \frac{\partial \phi_i}{\partial \beta} f_2(V, \beta, \dot{\psi}) - \frac{\partial \phi_i}{\partial \dot{\psi}} f_3(V, \beta, \dot{\psi}). \end{aligned} \quad (29)$$

Consider the control input

$$T_i = T_i^{\text{eq}} + I_w \hat{v}_i, \quad (30)$$

where

$$T_i^{\text{eq}} = f_{ix} r + I_w \left(\frac{\partial \phi_i}{\partial V} f_1 + \frac{\partial \phi_i}{\partial \beta} f_2 + \frac{\partial \phi_i}{\partial \dot{\psi}} f_3 \right). \quad (31)$$

The control component T_i^{eq} is referred to as the *equivalent control*. Taking $T_i = T_i^{\text{eq}}$ results in $\dot{\tilde{z}}_i = 0$ and ensures that the vehicle's states will remain in the *sliding manifold* $\tilde{z}_i = 0$. Equations (29), (30) and (31) yield

$$\dot{\tilde{z}}_i = \hat{v}_i, \quad i = F, R. \quad (32)$$

Finally, we take

$$\hat{v}_i = -\lambda_i \text{sat}(\tilde{z}_i), \quad \lambda_i > 0, \quad i = F, R. \quad (33)$$

It has been shown that the control (33) stabilizes (32) [17]. In fact, all trajectories starting off the *sliding manifold* $\tilde{z}_i = 0$ will reach it in finite time under the control input (30).

A. Sliding Mode Control Implementation

We consider two steady-state equilibrium points, namely, cases (a) and (b) from Table II. Both cases correspond to unstable equilibria along the same path radius, negotiated at the same speed. Case (a) is a steady-state condition of moderate vehicle sideslip angle, while case (b) is one of excessive slip angle.

The initial conditions in case (a) are:

$$V(0) = 1.2 V^{\text{ss}}, \quad \beta(0) = 2 \beta^{\text{ss}}, \quad \dot{\psi}(0) = 1.2 \dot{\psi}^{\text{ss}}, \quad (34)$$

whereas in case (b):

$$V(0) = 1.2 V^{\text{ss}}, \quad \beta(0) = \beta^{\text{ss}}/2, \quad \dot{\psi}(0) = 1.2 \dot{\psi}^{\text{ss}}. \quad (35)$$

In addition, we consider initial wheel speeds $\omega_F(0)$ and $\omega_R(0)$, such that the initial longitudinal slip at the front and rear wheels are both zero (pure rolling). The controller (30) is implemented in both cases with $\lambda_i = 1000$, ($i = F, R$). The parameters of the vehicle model used are the same as in Section V-A.

The resulting trajectories for the two simulation scenarios are shown in Fig. 2. The vehicle states and control inputs for the simulation cases (a) and (b) are shown in Figs. 3 and 4, respectively. We observe that the controller successfully stabilizes the vehicle with respect to both equilibria in the presence of significant perturbations of the initial states.

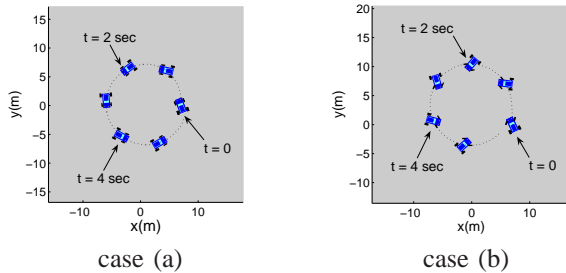


Fig. 2. Steady-state cornering stabilization via sliding mode control

VII. INCORPORATING SUSPENSION DYNAMICS

In this section we implement the same controller using a vehicle model of increased fidelity. In particular, we introduce a single-track model with suspension dynamics, and demonstrate the performance of the controller in the same simulation scenarios as in the previous section.

Let z be the vertical displacement of the center of gravity of the vehicle and θ the pitch angle of the suspended mass. The dynamics of the vertical translation and pitch rotation motions of the suspended mass are described by the following equations

$$m\ddot{z} = f_{Fz} + f_{Rz} - mg, \quad (36)$$

$$I_y\ddot{\theta} = f_{Rz}\ell_R \cos \theta - f_{Fz}\ell_F \cos \theta - \Sigma f_{Rx}(h+z) - \Sigma f_{Fx}(h+z), \quad (37)$$

where I_y is the moment of inertia of the vehicle about the the y body axis, h is the vertical distance of the C.M. from the ground in an equilibrium state where $z = 0$, and Σf_{ix} ($i = F, R$) is the projection of the total friction force of each wheel on the x body axis.

Given the vertical displacement of the C.M. z , and the pitch angle θ , the normal load of each wheel is given by

$$f_{Fz} = f_{Fz}^o - K_F \Delta z_F - C_F \Delta \dot{z}_F,$$

$$f_{Rz} = f_{Rz}^o - K_R \Delta z_R - C_R \Delta \dot{z}_R,$$

where

$$\Delta z_R = z + \ell_R \sin \theta, \quad \Delta z_F = z - \ell_F \sin \theta,$$

$$\Delta \dot{z}_R = \dot{z} + \dot{\theta} \ell_R \cos \theta, \quad \Delta \dot{z}_F = \dot{z} - \dot{\theta} \ell_F \cos \theta,$$

and f_{Fz}^o , f_{Rz}^o are the static normal loads on the front and rear wheels respectively.

We present simulation results of the implementation of the sliding mode control law of Section VI using the single-track model with suspension dynamics (21)-(23), (27), (36) and (37). The parameters of the vehicle model used are the same as in Section V-A. In addition, we use $K_F = K_R = 5000$ N/m, $C_F = C_R = 1000$ Ns/m and $I_y = 2741.9$ kgm². We consider the same simulation scenarios as in Section VI-A. In addition, we assume zero initial vertical displacement and velocity and zero pitch angle and pitch rate ($z(0) = \dot{z}(0) = 0$, $\theta(0) = \dot{\theta}(0) = 0$). The vehicle states and control inputs for the simulation cases (a) and (b) are shown in Figs. 3 and 4 respectively. We observe that the controller successfully stabilizes the vehicle model with suspension dynamics to the steady-state cornering conditions derived using the simplified single-track model.

VIII. CONCLUSIONS

In this work we studied the control of wheeled vehicles in extreme operating conditions. We explicitly derived steady-state cornering conditions for a vehicle operating in the nonlinear tire region. The resulting trajectories included cases of aggressive sideslip angle similar to driving techniques used by expert rally drivers. We also demonstrated that stabilization of these extreme steady-states may be achieved using only longitudinal (accelerating/braking) control. Use of longitudinal control to stabilize the vehicle dynamics during cornering was motivated by similar race driving techniques (e.g. “left-foot-braking”). While the steady-states and stabilizing controller design was based on a low order single-track vehicle model, the controller’s performance was validated by implementation using a model of higher level

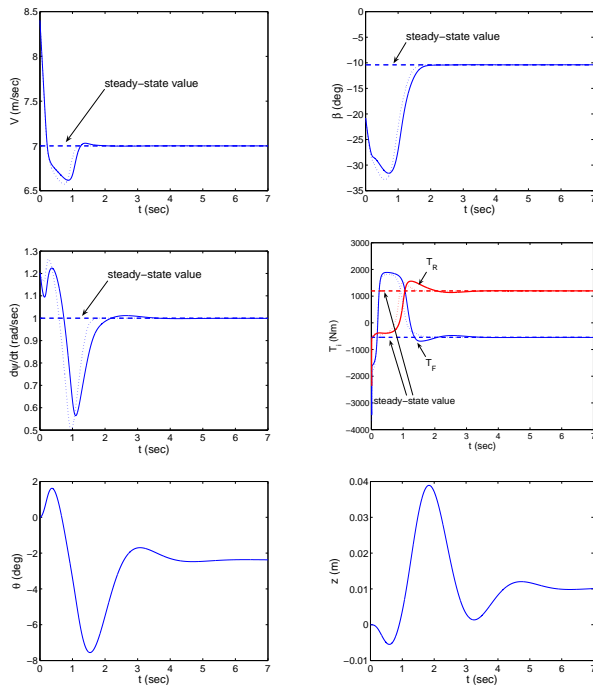


Fig. 3. Vehicle states and torque control inputs during stabilization of case (a). The dotted lines correspond to the response of the single-track model (21)-(23), (27). The solid lines correspond to the single track model model with suspension dynamics (36) and (37).

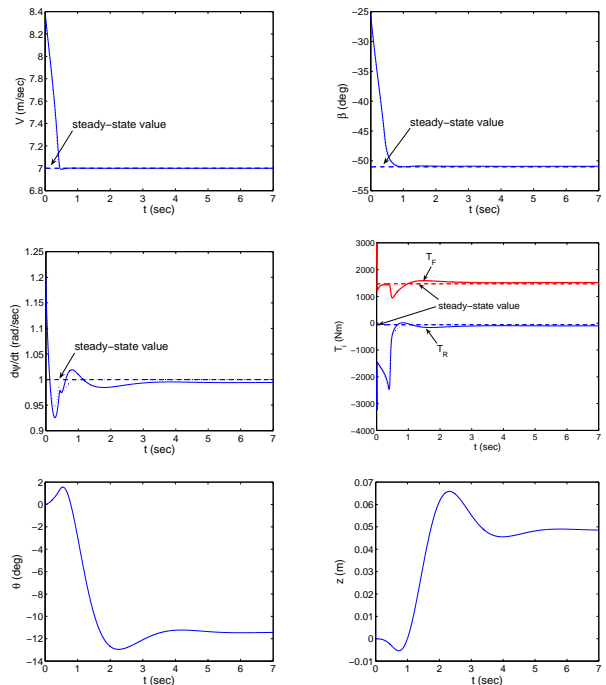


Fig. 4. Vehicle states and torque control inputs during stabilization of case (b). The dotted lines correspond to the response of the single-track model (21)-(23), (27). The solid lines correspond to the single track model model with suspension dynamics (36) and (37).

of detail. The extension of these results using vehicle models of increasing fidelity (e.g., four wheel models incorporating lateral load transfer effects), as well as the implementation of the controller using an actual autonomous vehicle platform will be addressed in the immediate future.

IX. ACKNOWLEDGMENTS

The work of the first author was supported by a Marie Curie International Reintegration Grant within the 7th European Community Framework Programme and a Brunel University BRIEF award. The work of the second author was supported by ARO award W911NF-07-1-0499. The work of the third author was supported by ARO award no W911NF-05-1-0331 and NSF GOALI award no CMMI-0727768.

REFERENCES

- [1] A. T. van Zanten, R. Erhardt, and G. Landesfeind, K. Pfaff, "Vehicle stabilization by the vehicle dynamics control system ESP," in *IFAC Mechatronic Systems*, Darmstadt, Germany, 2000, pp. 95–102.
- [2] J. Ackermann, "Robust control prevents car skidding," *IEEE Control Systems Magazine*, vol. 17, pp. 23–31, 1997.
- [3] K. Yoshimoto, H. Tanaka, and S. Kawakami, "Proposal of driver assistance system for recovering vehicle stability from unstable states by automatic steering," in *Proceedings of the IEEE International Vehicle Electronics Conference*, Changchun, China, September 6-9 1999.
- [4] A. Hac and M. Bodie, "Improvements in vehicle handling through integrated control of chassis systems," *International Journal of Vehicle Design*, vol. 29, no. 1.
- [5] A. Trachtler, "Integrated vehicle dynamics control using active brake steering and suspension systems," *International Journal of Vehicle Design*, vol. 36, no. 1, pp. 1–12, 2004.

- [6] J. Wei, Y. Zhuoping, and Z. Lijun, "Integrated chassis control system for improving vehicle stability," in *Proceedings of the IEEE International Conference on Vehicular Electronics and Safety*, Shanghai, China, December 6-9 2006.
- [7] F. Tahami, R. Kazemi, and S. Farhanghi, "A novel driver assist stability system for all-wheel-drive electric vehicles," *IEEE Transactions on Vehicular Technology*, vol. 52, no. 3, pp. 683–692, May 2003.
- [8] D. Kim, S. Hwang, and H. Kim, "Vehicle stability enhancement of four-wheel-drive hybrid electric vehicle using rear motor control," *IEEE Transactions on Vehicular Technology*, vol. 57, no. 2, pp. 727–735, March 2008.
- [9] T. Gillespie, *Fundamentals of Vehicle Dynamics*. Warrendale PA USA: Society of Automotive Engineers SAE International, 1992.
- [10] E. Velenis, P. Tsiotras, and J. Lu, "Modeling aggressive maneuvers on loose surfaces: The cases of trail-braking and pendulum-turn," in *Proceedings of the 2007 European Control Conference*, Kos, Greece, July 2-5 2007.
- [11] —, "Modeling aggressive maneuvers on loose surfaces: Data analysis and input parameterization," in *Proceedings of the 2007 Mediterranean Conference on Control and Automation*, Athens, Greece, June 27-29 2007.
- [12] —, "Trail-braking driver input parameterization for general corner geometry," in *Proceedings of the SAE Motorsports Engineering Conference*, Concord, NC, USA, December 2-4 2008.
- [13] —, "Optimality properties and driver input parameterization for trail-braking cornering," *European Journal of Control*, vol. 14, no. 4, pp. 308–320, July-August 2008.
- [14] E. Ono, S. Hosoe, H. Tuan, and S. Doi, "Bifurcation in vehicle dynamics and robust front wheel steering control," *IEEE Transactions on Control Systems Technology*, vol. 6, no. 3, pp. 412–420, May 1998.
- [15] E. Frazzoli, "Discussion on "Optimality Properties and Driver Input Parameterization for Trail-Braking Cornering"," *European Journal of Control*, vol. 14, no. 4, July-August 2008.
- [16] E. Bakker, L. Nyborg, and H. Pacejka, "Tyre modelling for use in vehicle dynamics studies," 1987, SAE Paper No. 870421.
- [17] H. Khalil, *Nonlinear Systems, 2nd edition*. Upper Saddle River, New Jersey: Prentice Hall, 1996.